

# A phenomenological spin-orbit three-body force

A. Kievsky\*

*Department of Physics and Astronomy, University of North Carolina at Chapel Hill, NC 27599-3255, USA and Triangle Universities Nuclear Laboratory, Durham, NC 27708, USA*

## Abstract

In order to improve the description of the N-d vector analyzing powers  $A_y$  and  $iT_{11}$  (the so-called  $A_y$  puzzle) a spin-orbit three-body force has been introduced. The  $\mathbf{L} \cdot \mathbf{S}$  term in the  $NN$  potential has been modified including a two-parameter three-body function depending on the hyperradius  $\rho$ . The modification has been performed in channels where the pair of nucleons  $(i, j)$  are coupled to spin  $S_{ij} = 1$  and isospin  $T_{ij} = 1$ . Calculations have been done in the energy region from  $E_{lab} = 648$  keV up to  $E_{lab} = 10$  MeV. A noticeable improvement in the description of the polarization observables has been obtained.

## I. INTRODUCTION

In the standard description of light nuclei as composed of structureless nucleons, three-nucleon forces (3NF's) play an important role. The simple assumption of nucleons interacting through a pairwise  $NN$  potential fails to reproduce the experimental binding energies. This suggests that the model has to be extended to include many-body forces in the potential energy. First derivations of 3NF's are based on two-pion exchange involving a  $\Delta$  excitation. The most often used potentials of this kind are the Tucson-Melbourne (TM) [1], the Brazil

---

\*Permanent address: Istituto Nazionale di Fisica Nucleare, Via Buonarroti 2, 56100 Pisa, Italy

(BR) [2] models, and the Urbana (UR) [3] model which also includes a central phenomenological repulsive term with no spin-isospin structure. In practical applications, the chosen 3NF is adjusted to reproduce the  $A = 3, 4$  binding energies. When the calculations are extended to describe bound states in  $p$ -shell nuclei, a persistent underbinding is observed in the mass region with  $A = 5 - 8$  [4]. In particular, several excited states are not well reproduced indicating that the 3NF could contain a more complicate structure.

A different problem has been observed in N-d scattering at low energies. The calculated vector analyzing powers  $A_y$  and  $iT_{11}$  show an unusual large discrepancy with the experimental data [5,6]. Attempts to improve the description of these observables with the inclusion of a two-pion three-nucleon force ( $2\pi$ -3NF) were unsuccessful [5-8]. This discrepancy has been called the  $A_y$  puzzle since it is, by far, the largest disagreement observed in the theoretical description of the three-nucleon system at low energies. Recently, it has been shown that the puzzle is not limited to the three-nucleon system but a similar problem appears in the calculation of  $A_y$  in  $p$ - $^3\text{He}$  scattering [9]. The  $A_y$  puzzle could be also a signal for different forms in the three-body potential [10,11]

In ref. [6] p-d and n-d scattering have been studied below the deuteron breakup. Using the experimental data for cross section and vector and tensor analyzing powers at  $E_{lab} = 2.5$  and 3.0 MeV from Shimizu et al. [12], it was possible to perform a phase-shift analysis (PSA) and to compare the results to the theoretical phases. The conclusion was that small differences in the  $P$ -wave parameters are responsible for the large disagreement in  $A_y$  and  $iT_{11}$ . It is a general feature that all realistic  $NN$  potentials underpredict the splitting in the  $^4P_J$  phases and the magnitude of the  $\epsilon_{3/2-}$  mixing parameter. When one of the  $2\pi$ -3NF's is included in the Hamiltonian there is not an appreciable reduction of the discrepancy, giving in some cases a poorer description. In fact, the inclusion of the  $2\pi$ -3NF tends to reduce the splitting in  $^4P_J$  and to slightly increase  $\epsilon_{3/2-}$ . These two opposite effects almost cancel each other in the construction of  $A_y$  and  $iT_{11}$ . The operator's form of these particular models of 3NF's does not include  $\mathbf{L} \cdot \mathbf{S}$  terms which are to a large extent responsible for the splitting in the  $P$ -waves parameters.

In the present paper a phenomenological spin-orbit three-nucleon force (SO-3NF) is introduced in order to study its effect on the N-d vector analyzing powers  $A_y$  and  $iT_{11}$  at low energies. The  $\mathbf{L} \cdot \mathbf{S}$  term in the  $NN$  potential has been modified including a two-parameter three-body function depending on the hyperradius  $\rho$ . The two parameters are related to the strength and range of the force and they have been fixed with the intention to improve the description of  $A_y$  and  $iT_{11}$  at  $E_{lab} = 3.0$  MeV, just below the deuteron breakup. Three different sets of parameters have been considered and, accordingly, used to calculate scattering observables from  $E_{lab} = 648$  keV up to  $E_{lab} = 10$  MeV. The SO-3NF has been introduced in channels where the pair of nucleons  $(i, j)$  are coupled to spin  $S_{ij} = 1$  and isospin  $T_{ij} = 1$ . At the level of the two-nucleon ( $2N$ ) system this channel is related to scattering in odd waves. In N-d scattering the  ${}^4P_J$  parameters and hence  $A_y$  and  $iT_{11}$  are very sensitive to the force in this particular channel. On the other hand its effect on the binding energy of the three-nucleon system is very small. This is the opposite behavior from that produced by the  $2\pi$ -3NF which gives the main contribution in the  $J = 1/2^+$  state and has small influence on the vector observables. Therefore these two different classes of 3NF's are to some extent complementary and can be studied separately.

The calculations of the N-d scattering observables presented here in the following at different energies have been done using the Pair Correlated Hyperspherical Harmonic (PHH) [13] basis. In this method the wave function of the system is expanded in terms of correlated basis elements and the description of the system proceeds via a variational principle. Bound states are obtained using the Rayleigh-Ritz variational principle whereas scattering states are obtained using the generalized Kohn variational principle. This technique has been extensively discussed in refs. [7,14,15] for energies below the deuteron breakup threshold and, very recently, also applied to energies above the breakup threshold [16,17].

The paper is organized as follows. In Sec. II the two parameter spin-orbit three-body force is introduced. In Sec. III the polarization observables as well as the binding energy of  ${}^3\text{He}$  are studied for specific values of these parameters. The conclusions and perspectives are given in the last section.

## II. A TWO-PARAMETER SPIN-ORBIT THREE-BODY FORCE

Disregarding for the moment the presence of three-nucleon forces, the potential energy operator of the three-nucleon system is

$$V_{3N} = \sum_{i < j} V_{2N}(i, j) , \quad (1)$$

where  $V_{2N}$  is the  $NN$  interaction that, in general, is constructed by fitting the  $2N$  scattering data and the deuteron properties. Recently, several potential models have been determined including explicitly charge dependence which describe the  $2N$  data with a  $\chi^2$  per datum  $\approx 1$ . Here we will refer to the Argonne AV18 interaction, which is one of these new generation potentials [18]. The nuclear part of the AV18 potential consists of a sum over 18 different terms. The first 14 terms are charge independent whereas the four additional operators introduce charge symmetry breaking. Each of the first 14 terms includes a projector  $P_{ST}(ij)$  onto the spin-isospin states  $S, T$  of particles  $(i, j)$  multiplied by one of the following operators,  $\mathcal{O}^p = 1, S_{12}, \mathbf{L} \cdot \mathbf{S}, L^2, (\mathbf{L} \cdot \mathbf{S})^2$ . The strength of each term is given by a scalar function  $v_{ST}^p(r_{ij})$  depending on the relative distance between particles  $(i, j)$ . For example the  $\mathbf{L} \cdot \mathbf{S}$  interaction between particles  $(i, j)$  is defined in the two channels with isospin  $T_{ij} = 0, 1$  and spin  $S_{ij} = 1$  and is given by the functions  $v_{10}^{ls}(r_{ij})$  and  $v_{11}^{ls}(r_{ij})$ , respectively.

In the three-nucleon system odd-parity scattering states are directly related to the potential in channels where particles  $(i, j)$  are coupled to  $S_{ij} = 1, T_{ij} = 1$ . In particular here we are interested in the  $\mathbf{L} \cdot \mathbf{S}$  term and its relation to the vector observables  $A_y$  and  $iT_{11}$ . Limiting the discussion to the  $\mathbf{L} \cdot \mathbf{S}$  interaction in this particular channel, the corresponding term in the three-nucleon potential energy is

$$V_{3N}^{ls} = \sum_{i < j} v_{11}^{ls}(r_{ij}) \mathbf{L}_{ij} \cdot \mathbf{S}_{ij} P_{11}(ij) . \quad (2)$$

At this point we can conjecture that the presence of the third nucleon (particle  $k$ ) could modify the interaction, introducing in the function  $v_{11}^{ls}$  a dependence on the distances between the third nucleon  $k$  and particles  $(i, j)$ . Accordingly, the above interaction transforms to

$$V_{3N}^{ls} = \sum_{i<j} \frac{1}{2} [w_{11}^{ls}(r_{ijk}) \mathbf{L}_{ij} \cdot \mathbf{S}_{ij} + \mathbf{L}_{ij} \cdot \mathbf{S}_{ij} w_{11}^{ls}(r_{ijk})] P_{11}(ij) , \quad (3)$$

where  $r_{ijk}$  is a scalar function of the three interparticle distances  $r_{ij}, r_{jk}, r_{ki}$ . The symmetric form has been introduced since, in general, the  $\mathbf{L} \cdot \mathbf{S}$  operator does not commute with an operator depending on  $r_{ijk}$ . Different forms are possible for the three-body interaction  $w_{11}^{ls}(r_{ijk})$  provided that  $w_{11}^{ls}(r_{ijk}) \rightarrow v_{11}^{ls}(r_{ij})$  when  $r_{ik}, r_{jk} \rightarrow \infty$ . A simple two-parameter form that we are going to analyze here is

$$w_{11}^{ls}(r_{ijk}) = v_{11}^{ls}(r_{ij}) + W_0 e^{-\alpha \rho} , \quad (4)$$

where the hyperradius  $\rho$  is

$$\rho^2 = \frac{2}{3} (r_{12}^2 + r_{23}^2 + r_{31}^2) \quad (5)$$

and  $W_0$  and  $\alpha$  are parameters characterizing the strength and range of the three-body term. When the dependence in the scalar function  $r_{ijk}$  is limited to  $r_{ij}$  and  $\rho$ , the operators  $w_{11}^{ls}(r_{ij}, \rho)$  and  $\mathbf{L}_{ij} \cdot \mathbf{S}_{ij}$  commute. Accordingly, the spin-orbit force becomes

$$V_{3N}^{ls} = \sum_{i<j} v_{11}^{ls}(r_{ij}) \mathbf{L}_{ij} \cdot \mathbf{S}_{ij} P_{11}(ij) + W_0 e^{-\alpha \rho} \sum_{i<j} \mathbf{L}_{ij} \cdot \mathbf{S}_{ij} P_{11}(ij) . \quad (6)$$

Replacing this term in eq.(1) and including now also the  $2\pi$ -3NF, the final form for the three-nucleon potential energy to be used in the present work is

$$V_{3N} = \sum_{i<j} V_{2N}(i, j) + \sum_{i<j<k} W_{3N}^{ls}(i, j, k) + \sum_{i<j<k} W_{3N}^{2\pi}(i, j, k) . \quad (7)$$

The  $W_{3N}^{ls}$  term is the phenomenological spin-orbit force defined in the second term of eq.(6); for the  $W_{3N}^{2\pi}$  term the discussion will be limited to the Urbana force.

The choice of the two-parameter exponential form in the definition of  $w_{11}^{ls}$  (see eq.(4)) is arbitrary and was selected in order to make a phenomenological representation of a 3NF containing a spin-orbit interaction. The hyperradial dependence is the simplest scalar function depending on the three-interparticle distances which has the property of commuting with the spin-orbit operator. These choices, driven by simplicity, have been made in order

to focus on the spin-orbit operator and its relation to  $A_y$  and  $iT_{11}$  in p-d scattering. The numerical values for the constants  $W_0, \alpha$  are discussed in the next section.

In principle, the argument used to introduce the scalar function  $w_{11}^{ls}(r_{ijk})$  as a modification of the function  $v_{11}^{ls}(r_{ij})$  due to the presence of particle  $k$ , could be extended to the other functions  $v_{ST}^p(r_{ij})$  of the  $NN$  potential. This leads to a three-body force with an hybrid form in which nucleons  $(i, j)$  interact with the same operator's structure of the  $NN$  potential but with scalar functions depending on the interparticle distances of the three nucleons  $(i, j, k)$ . The original function  $v_{ST}^p(r_{ij})$  must be recovered when nucleon  $k$  is at  $\infty$ . In the present work we are limiting the argument to one specific term and trying to relate its parametrization to the two vector observables  $A_y$  and  $iT_{11}$ .

### III. N-D SCATTERING CALCULATIONS WITH THE SO-3NF

The inclusion of the SO-3NF has been done with the hope of improving the description of  $A_y$  and  $iT_{11}$  without destroying the agreement already observed for the cross section and tensor observables. At energies below the deuteron breakup, measurements for tensor and vector observables exist for p-d scattering at  $E_{lab} = 648$  keV [10] and at  $E_{lab} = 2.5$  MeV and 3.0 MeV [12,19]. The 648 keV data set is at the lowest energy at which these measurements have been made. The other two sets of measurements lie just below the deuteron breakup. Theoretical calculations using the AV18 potential underpredict  $A_y$  and  $iT_{11}$  of about 30%. Comparisons to phase-shift and mixing parameters extracted from PSA performed at these three energies [6,10,19] show the aforementioned insufficient splitting in the  ${}^4P_J$  phase shifts as well as an underpredicted  $\epsilon_{3/2-}$ . Calculations using the AV18+UR potential essentially do not change these findings. The almost constant underprediction in the vector polarization observables (in percentage) and the fact that the inclusion of the  $2\pi$ -3NF's does not increase the splitting in  ${}^4P_J$  is a motivation for considering new additional forms for the three-body potential. The selection of the  $\mathbf{L} \cdot \mathbf{S}$  operator is a natural choice since when applied to the  ${}^4P_J$  state it acts with opposite sign in the states  $J = 1/2^-$  and  $J = 5/2^-$ , tending to increase

the splitting.

Three different choices of the exponent  $\alpha$  in the hyperradial spin-orbit interaction defined in eq.(4) have been selected with the intention of constructing forces with different ranges. The strength  $W_0$  has been adjusted in each case in an attempt to improve the description of the vector observables. The analysis has been performed at  $E_{lab} = 3.0$  MeV. The selected ranges are  $\alpha = 0.7, 1.2, 1.5$  fm $^{-1}$ , so as to simulate a long, medium and short range force. The corresponding values for the depth are  $W_0 = -1, -10, -20$  MeV. The calculations have been performed using the nuclear part of AV18 plus the Coulomb interaction. The  $2\pi$ -3NF has been disregarded at the present stage since its contribution to the description of the vector observables is small.

The results for the proton and neutron analyzing powers  $A_y$  and the deuteron analyzing power  $iT_{11}$  are given in Fig.1 together with the experimental data of ref. [12,20]. The four curves correspond to the AV18 potential and the three different choices for the parameters  $(\alpha, W_0)$ . The dotted line is the AV18 prediction and shows the expected discrepancy. The solid line corresponds to the AV18 plus the long range force (AV18+LS1), the long-dashed line to the AV18 plus the medium range force (AV18+LS2) and the dotted-dashed line to the AV18 plus the short range force (AV18+LS3). The inclusion of the spin-orbit force improves the description of the vector observables, although there is a slightly different sensitivity in  $A_y$  and  $iT_{11}$ . The AV18+LS1 curve is slightly above the data, especially for  $iT_{11}$ . The AV18+LS2 curve is slightly below (above) the data in  $A_y$  ( $iT_{11}$ ). The AV18+LS3 curve is slightly below the data especially for  $A_y$ . In the bottom panel of Fig.1 the n-d analyzing power has been calculated using the same potential models as before. Again, there is an improvement in the description of  $A_y$  equivalent to that one obtained in the p-d case. In Fig.2 the tensor analyzing powers  $T_{20}, T_{21}, T_{22}$  are shown at the same energy and compared to the data of ref. [12]. The inclusion of the SO-3NF has no appreciable effect and the four curves are practically on top of each other. These observables are not very sensitive to the splitting in  $^4P_J$ -waves. They are sensitive to scattering in  $D$ -waves and higher partial waves, which are only weakly distorted by the SO-3NF.

Before extending the calculations to other energies the analysis of the binding energy of  ${}^3\text{He}$  deserves some attention. We expect that the inclusion of the  $W_{3N}^{ls}$  term will produce only a small distortion in the bound state due to the low occupation probability of channels with  $S_{ij} = 1$  and  $T_{ij} = 1$ . This is corroborated by the calculations shown in table I. The binding energy, the kinetic energy and the  $S'$ -,  $D$ -, and  $P$ -wave probabilities are given for the different potential models. The AV18 and the AV18+UR interactions have been considered. The  $2\pi$ -3NF of Urbana has been now taken into account since it produces large effects in the bound state. Calculations have been done for these two potentials with and without the inclusion of the three different choices for the SO-3NF. Its inclusion produces a small repulsion which in any case is not greater than 50 keV, with all the other mean values modified very little. The force with the longest range produces very tiny effects due to its very small strength. The other two forces produce slightly greater, and similar, modifications. We can conclude that the structure of the three-body bound state remains essentially unaffected by the spin-orbit 3NF with the ranges and strengths considered.

The analysis of the bound state is important since changes in  $A_y$  and  $iT_{11}$  of the size shown in Fig.1 could, in principle, be obtained with modified forms of the  $2\pi$ -3NF's. But, in general, these modifications are not anymore compatible with a correct description of the bound state. This is not the case for the spin-orbit 3NF we are considering. Therefore, we can extend the calculations to other energies based in the fact that the new model makes a selective and appreciable effect only in the vector observables. Calculations have been done at  $E_{lab} = 648$  keV and 2.5 MeV. The results for  $A_y$  and  $iT_{11}$  are shown in Fig.3 and compared to the experimental data of refs. [10,12]. Again a remarkable improvement in the description of both observables is obtained. At the lowest energy the AV18+LS1 model seems to be more effective because of its long range whereas for the other two ranges the centrifugal barrier plays some role. The results at  $E_{lab} = 2.5$  MeV have the same characteristics as those at 3.0 MeV.

In table 2 we compare results for the  $P$ -waves parameters at  $E_{lab} = 2.5$  and 3.0 MeV. Again, different cases using the AV18 potential with and without the inclusion of the spin-



orbit 3NF have been considered. In the last column the parameters corresponding to the PSA from ref. [6] are given for the sake of comparison. In the three cases the SO-3NF increases the splitting of the  ${}^4P_J$  phases. The phases  ${}^4P_{1/2}$  and  ${}^4P_{5/2}$  and the mixing parameter  $\epsilon_{3/2-}$ , which play a major role in the description of the vector observables, are now in much better agreement with the PSA values. It was not obvious from the beginning that with two parameters  $(\alpha, W_0)$ , it would be possible to increase the difference  $\Delta P = {}^4P_{5/2} - {}^4P_{1/2}$  in the measure suggested by the PSA, together with a change in  $\epsilon_{3/2-}$  in the expected direction and magnitude. At the three energies the change in  $\epsilon_{3/2-}$  was observed to happen in the correct direction. Not all parameters are closer to the PSA values after including the SO-3NF. For example  ${}^4P_{3/2}$  has slightly changed in the opposite direction to that suggested by the PSA. But the final result in the description of the observables was found always to produce an improvement.

In order to complete the study of the SO-3NF the extension to p-d calculations above the breakup channel is now considered. This extension is not straightforward since when the breakup channel is open a correct description of the three outgoing nucleons has to be done. In particular, in the p-d case, the Coulomb interaction introduces difficulties that have been, and are at present, subject of intense investigation. Recently the PHH technique has been extended to describe p-d elastic scattering above the deuteron breakup [16,17]. The method is based on the use of the Kohn variational principle in its complex form [15] and it provides an accurate description of the polarization observables. In ref. [17] differential cross sections and vector and tensor analyzing powers at  $E_{lab} = 5$  and 10 MeV have been calculated using the AV18 interaction. In the present work, calculations have been done at the same two energies using the AV18 interaction with and without the SO-3NF. The results for  $A_y$  and  $iT_{11}$  are given in Fig.4 together with the experimental data from ref. [21] ( $E_{lab} = 5$  MeV) and ref. [22] ( $E_{lab} = 10$  MeV). Also at these energies we observe the same trend as before, both observables are now better described. The sensitivity to the different ranges is slightly different with the medium range model starting to be more effective. In fact, at 5 MeV the long and medium range curves overlap and at 10 MeV the splitting in the curves is now

reversed in that the upper curve corresponds to the medium range force.

Finally, let us extend the analysis of the effects of the SO-3NF to other observables at different energies. In Fig.5 the effects on the elastic cross section are shown in the energy interval from  $E_{lab} = 648$  keV up to  $E_{lab} = 10$  MeV. At each energy, the four curves corresponding to the different potential models are on top of each other. There is not enough sensitivity in this observable to changes in the phase-shift and mixing parameters of the magnitude introduced by the SO-3NF used. The tensor analyzing powers at  $E_{lab} = 5$  MeV and 10 MeV are shown in Fig.6. The effects on these observables are very small. The three curves corresponding to the AV18 plus the SO-3NF are practically superposed with slight differences with the AV18 curve (dotted line). In particular, the second minimum of  $T_{20}$  is slightly improved as well as the second maximum of  $T_{21}$ , whereas  $T_{22}$  is essentially unchanged.

In order to give a quantitative measure of the improvement introduced by the SO-3NF in the description of the data, a  $\chi^2$  (per datum) analysis is displayed in table III. The analysis includes the cross section, the two vector and the three tensor analyzing powers at  $E_{lab} = 648$  keV, 3 MeV, 5 MeV and 10 MeV. The data set has been taken from ref. [10,12,21-23]. The  $\chi^2$  per datum has been calculated using the theoretical predictions of the AV18 potential model with and without the inclusion of the SO-3NF. The cases corresponding to the three different choices of the strength and range parameters have been considered. From the table is clear the selective effect of the spin-orbit force on the vector observables. There is a dramatic improvement in terms of  $\chi^2$  in these observables, whos value is reduced by more than one order of magnitude in several cases. At each energy, the AV18+LS1 and AV18+LS2 potential models give the best description. At the first three energies both potential models reproduce the data reasonably well and with similar quality. At 10 MeV the obtained  $\chi^2$  per datum for  $A_y$  is very high in all cases. This is a consequence of the extremely small error bars in the data set at this particular energy. However, the  $\chi^2$  has been improved by a factor of  $\approx 25$  going from AV18 to AV18+LS2 and a further reduction could be obtained with a fine tune of the strength and range parameters  $W_0, \alpha$ .

Looking at the differential cross section, in all cases the  $\chi^2$  per datum is a large number and it changes very little when the SO-3NF is included. There is a sensitivity to the  $^3\text{He}$  binding energy which is not well reproduced unless a  $2\pi$ -3NF is considered. For example, the value  $\chi^2 = 30.3$  at 3 MeV obtained with the AV18 potential reduces to  $\chi^2 = 4.0$  with the AV18+UR potential. In the case of the tensor observables the changes in terms of  $\chi^2$  when the SO-3NF is considered are moderated. There is a slight improvement in the description of  $T_{20}$  and  $T_{21}$ , whereas the reverse situation is seen in  $T_{22}$ .

#### IV. CONCLUSIONS

Elastic N-d scattering has been studied in the energy range from  $E_{lab} = 648$  keV to  $E_{lab} = 10$  MeV using a potential model which includes a spin-orbit three-nucleon interaction. This three-body potential was introduced as a “distortion” of the function  $v_{11}^{ls}(r_{ij})$  of the  $NN$  potential. This function gives the magnitude of the  $\mathbf{L} \cdot \mathbf{S}$  interaction in the channels where particles  $(i, j)$  are coupled to spin  $S_{ij} = 1$  and isospin  $T_{ij} = 1$  and was converted to a function  $w_{11}^{ls}(r_{ijk})$  depending on the three-interparticle distances  $r_{ij}, r_{jk}, r_{ki}$ . The condition on  $w_{11}^{ls}$  was that the interaction  $v_{11}^{ls}$  is recovered when the third particle is far from the other two. A phenomenological hyperradial exponential form depending on two parameters was used which fixes the range and strength of the three-body part of the interaction.

The choice of the  $\mathbf{L} \cdot \mathbf{S}$  operator acting on the  $S_{ij} = 1, T_{ij} = 1$  spin-isospin channels was based on the large effects it has in the description of the two vector observables  $A_y$  and  $iT_{11}$  in N-d scattering. The origin of this discrepancy lies in the too low splitting predicted by all realistic potential models for the  $^4P_J$  phase shifts. There is a close relation, due to the Pauli blocking, between scattering in  $^4P_J$ -waves and the interaction in this channel. Moreover the  $\mathbf{L} \cdot \mathbf{S}$  operator is attractive (repulsive) in the  $J = 1/2^-$  state ( $J = 5/2^-$  state), therefore increasing the splitting of these phases.

The study of the SO-3NF was done phenomenologically by fixing three different values for its range parameter  $\alpha$  and selecting the strength parameter  $W_0$  to provide a better description

of the vector observables. The energy at  $E_{lab} = 3.0$  MeV was chosen for this analysis and successively the three sets of parameters were used to describe the same observables at different energies. The difference between the curves obtained for the description of  $A_y$  and  $iT_{11}$  after including the spin-orbit force could be further reduced with a fine tuning of  $W_0$ . An important check was made resulting in the observation that the structure of the bound state and other observables, for example the tensor analyzing powers are not appreciably disturbed by this interaction. Moreover the n-d and p-d  $A_y$  are described equally well when the spin-orbit 3NF is included. This means that no additional charge-symmetry breaking effects are needed.

The use of this phenomenological SO-3NF improves the description of the vector observables in all the studied cases, from  $E_{lab} = 648$  keV to  $E_{lab} = 10$  MeV. The sensitivity of the observables to the range parameters is slightly different at the energies studied and there is not a definitive preference for one of them. Perhaps the set with the medium range parameter ( $\alpha = 1.2$  fm $^{-1}$ ,  $W_0 = -10$  MeV) gives on average the best description. A better evaluation about the simple hyperradial dependence introduced here because of its nice property of commuting with the  $\mathbf{L} \cdot \mathbf{S}$  operator, can be obtained only after extending the calculations to higher energies. The main conclusion of the present work is the identification of the  $\mathbf{L} \cdot \mathbf{S}$  force in the  $S_{ij} = 1$ ,  $T_{ij} = 1$  spin-isospin channel as one which can resolve the  $A_y$  puzzle. In addition, a simple model has been proposed to repair the discrepancy.

Further investigations, which are in progress, consist in the inclusion of the  $2\pi$ -3NF in the description of the scattering observables other than in the bound state, the extension of the calculations to higher energies and the study of the force in the four-body reaction p- $^3\text{He}$ . Whereas in the first case we can expect at most a small change of the two parameters ( $\alpha, W_0$ ), the two other studies will give more insight about the force. In particular, by studying the p- $^3\text{He}$  reaction the extension to heavier systems can be tested.

Finally, the possibility of introducing a dependence on the three interparticle distances in other NN functions  $v_{ST}^p(r_{ij})$ , as discussed at the end of Sec. II, deserves some attention. Disregarding other types of 3NF's, the modified potential energy between three nucleons

would be

$$V_{3N} = \sum_{i < j} \sum_{S,T} \sum_p \frac{1}{2} [w_{ST}^p(r_{ijk}) \mathcal{O}_{ij}^p + \mathcal{O}_{ij}^p w_{ST}^p(r_{ijk})] P_{ST}(ij) . \quad (8)$$

The original functions  $v_{ST}^p$  are recovered when nucleon  $k$  is far from the pair  $(i, j)$ . In addition, the symmetric form can be avoided if the three-body radial dependence is limited to the hyperradius, i.e.  $w_{ST}^p(r_{ijk}) = w_{ST}^p(r_{ij}, \rho)$ . The next step is the parametrization of the functions  $w_{ST}^p$  with a number of parameters to be determined by a fit procedure. The maximum number of free parameters and the selection of the channels where the distorted functions are introduced are related to the observables included in the fit. For example, it would be impossible to reproduce simultaneously the binding energy of  ${}^3\text{He}$  and the vector analyzing powers in p-d scattering by modifying the potential only in channels with  $S_{ij} = 1, T_{ij} = 1$  and neglecting the  $2\pi$ -3NF. Conversely, this would be possible by extending the modification to other terms in channels with  $S_{ij} = 1, T_{ij} = 0$  or  $S_{ij} = 0, T_{ij} = 1$ .

### ACKNOWLEDGMENTS

I would like to thank the University of North Carolina at Chapel Hill and the Triangle Universities Nuclear Laboratory for hospitality and support during my stay in Chapel Hill, where this work was performed. Moreover, I would like to thank W. Tornow, E. Ludwig, H. Karwowski, C. Brune, L. Knutson and E. George as well as M. Viviani, S. Rosati and A. Fabrocini for useful discussions.

## REFERENCES

- [1] S. A. Coon *et al.*; Nucl. Phys. **A317**, 242 (1979); S. A. Coon and W. Glöckle, Phys. Rev. **C23**, 1790 (1981)
- [2] H. T. Coelho, T. K. Das and M. R. Robilotta; Phys. Rev. **C28**, 1812 (1983)
- [3] B. S. Pudliner *et al.*; Phys. Rev. Lett. **74**, 4396 (1995)
- [4] B. S. Pudliner *et al.*; Phys. Rev. **C56**, 1720 (1997); R. B. Wiringa; Nuc. Phys. **A631** 70c (1998)
- [5] H. Witała and W. Glöckle, Nucl. Phys. **A528**, 48 (1991); H. Witała, D. Hüber and W. Glöckle, Phys. Rev. **C49**, R14 (1994)
- [6] A. Kievsky *et al.*; Nucl. Phys. **A607**, 402 (1996)
- [7] A. Kievsky, M. Viviani, S. Rosati; Phys. Rev. **C52**, R15 (1995)
- [8] W. Glöckle *et al.*; Phys. Rep. **274**, 107 (1996)
- [9] M. Viviani, *XVIth European Conference on Few-Body Problems in Physics*, Autran 1998
- [10] C. R. Brune *et al.*, Phys. Lett. **B428**, 13 (1998)
- [11] D. Hüber and J. Friar, Phys. Rev. **C58**, 674 (1998)
- [12] S. Shimizu *et al.*, Phys. Rev. **C52**, 1193 (1995)
- [13] A. Kievsky, M. Viviani, S. Rosati; Nucl. Phys. **A551**, 241 (1993)
- [14] A. Kievsky, M. Viviani, S. Rosati; Nucl. Phys. **A577**, 511 (1994)
- [15] A. Kievsky; Nucl. Phys. **A624**, 125 (1997)
- [16] A. Kievsky, M. Viviani, S. Rosati; Phys. Rev. **C56**, 2987 (1997)
- [17] A. Kievsky, M. Viviani, S. Rosati; Phy. Rev. Let., in press

- [18] R. B. Wiringa, V. G. J. Stocks and R. Schiavilla; Phys. Rev. **C51**, 38 (1995)
- [19] L. D. Knutson, L. O. Lamm and J. E. McAninch, Phys. Rev. Lett. **71**, 3762 (1993)
- [20] J. E. McAninch, L. O. Lamm and W. Haeberli, Phys. Rev. **C50**, 589 (1994)
- [21] K. Sagara *et al.*, Phys. Rev. **C50**, 576 (1994); K. Sagara, private communication
- [22] F. Sperisen *et al.*; Nucl. Phys. **A422**,81 (1984)
- [23] A. Kievsky *et al.*, Phys. Lett. **B406**, 292 (1997), C. R. Brune, private communication.

## Table Captions

Table 1. The binding energy of  ${}^3\text{He}$  is shown together with the kinetic energy and the  $S'$ -,  $P$ - and  $D$ -wave probabilities. The AV18 and the AV18+UR potentials are considered with and without the spin-orbit 3NF for three choices for the parameters (see text).

Table 2. The  $P$ -waves phase shift and mixing parameters calculated at two different energies. The AV18 potential and three different sets for the parameters in the spin-orbit 3NF (see text) have been used. The results from the PSA of ref. [6] are given in column 6 for the sake of comparison.

Table 3.  $\chi^2$  per datum at four different energies calculated using the AV18 potential model with and without the three different parametrization of the SO-3NF. The data set has been taken from refs. [10,12,21–23]. The number in parenthesis is the number of data points.



## Figure Captions

Fig.1. The p-d and n-d analyzing power  $A_y$  and the deuteron analyzing power  $iT_{11}$  are shown at  $E_{lab} = 3.0$  MeV. The different curves correspond to the following potential models: AV18(dotted line), AV18+LS1 (solid line), AV18+LS2 (dashed line), AV18+LS3 (dotted-dashed line). The experimental data are from ref. [12] (p-d) and ref. [20] (n-d).

Fig.2. The tensor analyzing powers  $T_{20}, T_{21}, T_{22}$  at  $E_{lab} = 3.0$  MeV for the same potential model as Fig.1. The experimental data are from ref. [12].

Fig.3.  $A_y$  and  $iT_{11}$  at two different lab energies. The four curves correspond to the same potentials as in the previous figures. Experimental data are from ref. [10] at 648 keV and from ref. [12] at 2.5 MeV.

Fig.4. As in Fig.3 at two different energies above the deuteron breakup threshold. Experimental data are from ref. [21] at 5 MeV and from ref. [22] at 10 MeV.

Fig.5. The differential cross section at five different lab energies. At each energy the four curves corresponding to the AV18 potential with and without the SO-3NF overlap. Experimental points are from refs. [12,21,23].

Fig.6. The tensor analyzing powers at  $E_{lab} = 5$  MeV and 10 MeV. At each energy there are four curves corresponding to AV18 (dotted line), AV18+LS1 (solid line), AV18+LS2 (dashed line) and AV18+LS3 (dotted-dashed line).

TABLES

Potential	B(MeV)	T(MeV)	$P_{S'}$ (%)	$P_P$ (%)	$P_D$ (%)
AV18	-6.942	45.72	1.542	0.065	8.481
AV18+LS1	-6.929	45.66	1.546	0.064	8.456
AV18+LS2	-6.905	45.52	1.555	0.063	8.423
AV18+LS3	-6.905	45.52	1.556	0.063	8.427
AV18+UR	-7.768	50.25	1.251	0.132	9.262
AV18+UR+LS1	-7.751	50.17	1.255	0.131	9.233
AV18+UR+LS2	-7.718	49.99	1.264	0.129	9.190
AV18+UR+LS3	-7.718	49.97	1.265	0.129	9.194

TABLE I.

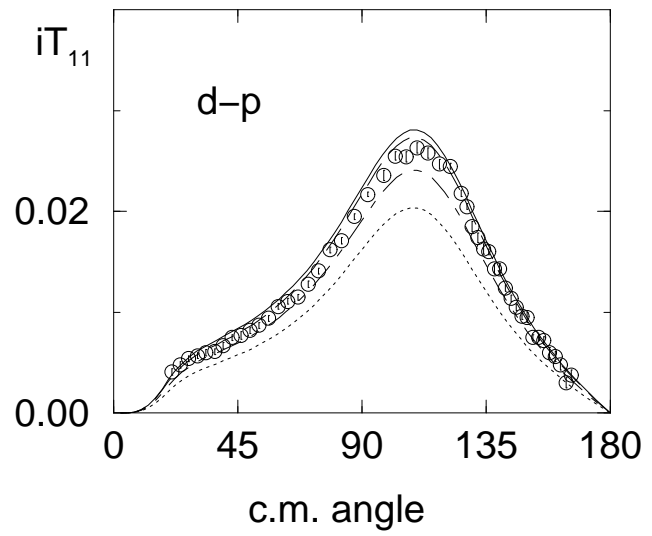
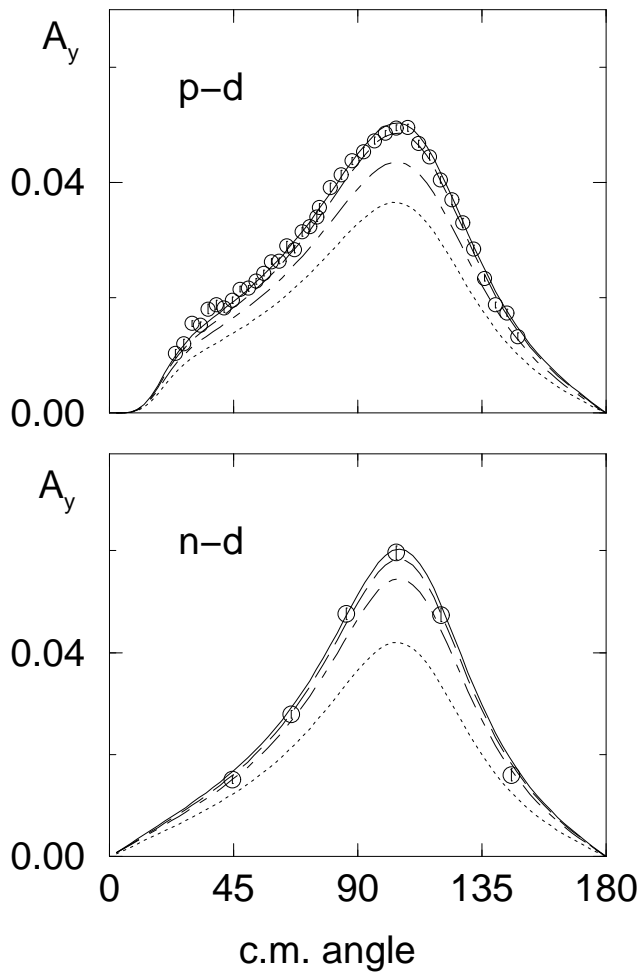
$E_{lab} = 3.0 \text{ MeV}$					
	AV18	AV18+LS1	AV18+LS2	AV18+LS3	PSA
${}^2P_{1/2}$	-7.36	-7.40	-7.38	-7.37	-7.41
${}^2P_{3/2}$	-7.12	-7.11	-7.12	-7.12	-7.18
${}^4P_{1/2}$	22.11	21.67	21.72	21.87	21.77
${}^4P_{3/2}$	24.23	24.10	24.14	24.18	24.30
${}^4P_{5/2}$	24.00	24.27	24.25	24.17	24.26
$\epsilon_{1/2-}$	5.72	5.62	5.62	5.66	5.70
$\epsilon_{3/2-}$	-2.22	-2.37	-2.33	-2.29	-2.46
$E_{lab} = 2.5 \text{ MeV}$					
	AV18	AV18+LS1	AV18+LS2	AV18+LS3	PSA
${}^2P_{1/2}$	-6.85	-6.88	-6.87	-6.86	-7.11
${}^2P_{3/2}$	-6.70	-6.67	-6.68	-6.68	-6.90
${}^4P_{1/2}$	20.10	19.70	19.75	19.87	19.89
${}^4P_{3/2}$	22.45	22.27	22.30	22.34	22.49
${}^4P_{5/2}$	21.84	22.08	22.07	22.00	22.14
$\epsilon_{1/2-}$	4.95	4.87	4.87	4.90	4.77
$\epsilon_{3/2-}$	-1.86	-2.01	-1.98	-1.94	-2.06

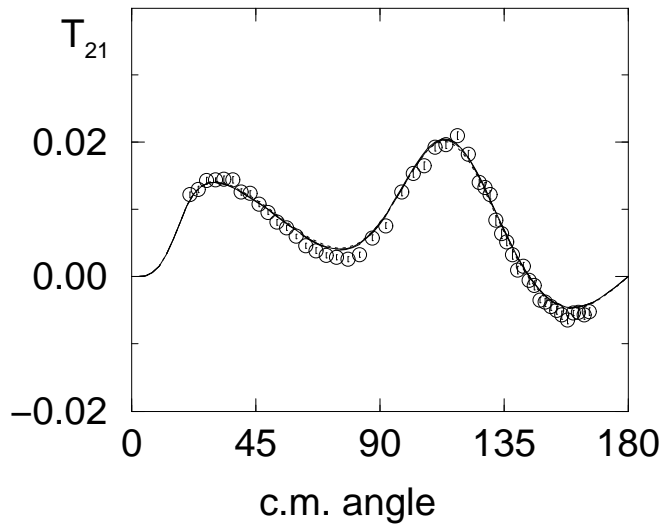
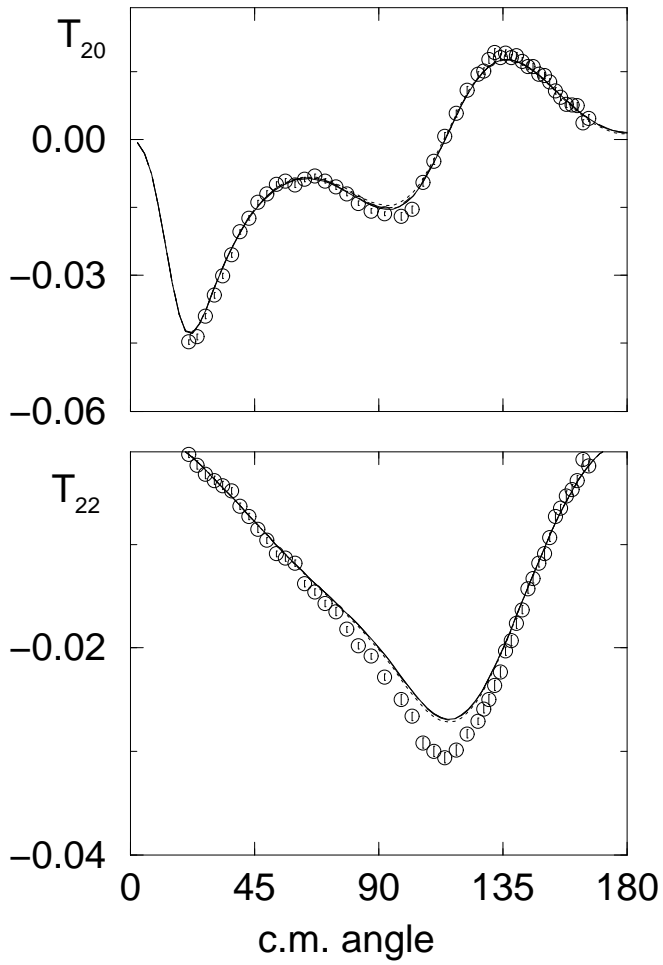
TABLE II.

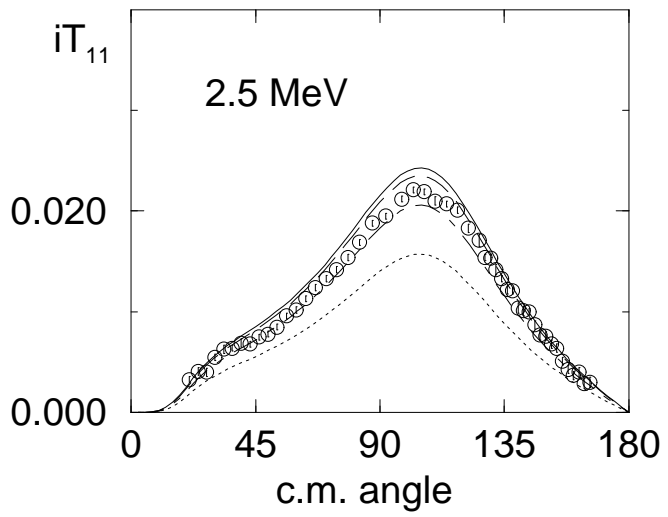
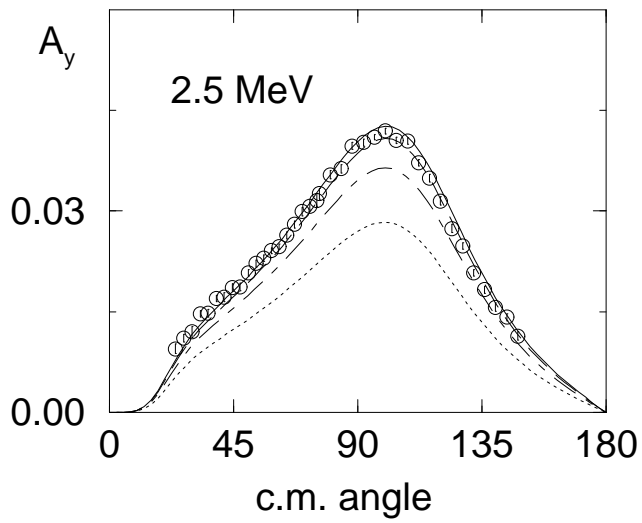
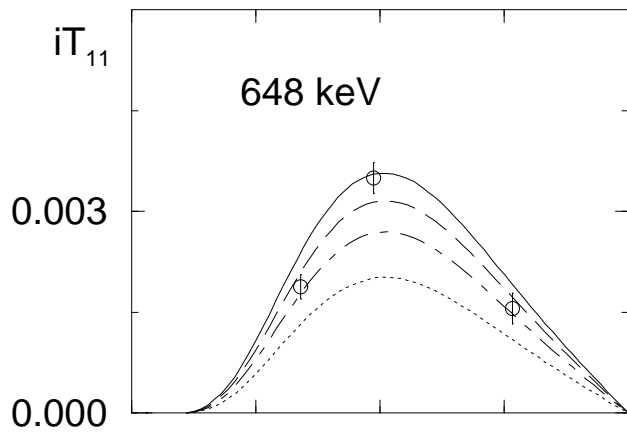
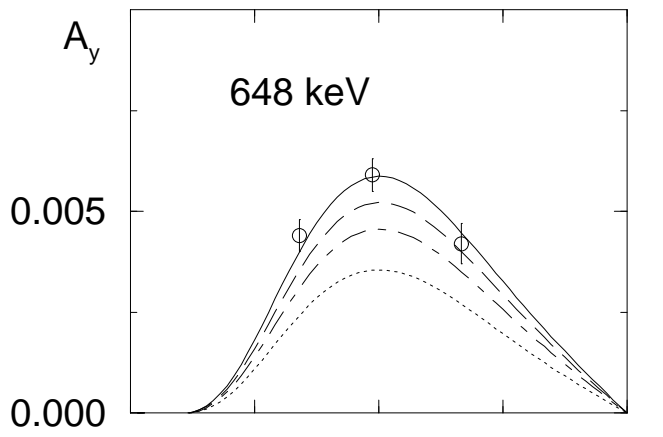
$E_{lab} = 648 \text{ keV}$	AV18	AV18+LS1	AV18+LS2	AV18+LS3
$\sigma$ (19)	38.5	39.5	41.0	41.5
$A_y$ (3)	22.7	0.4	2.6	8
$iT_{11}$ (3)	18.3	3.4	1.4	4.3
$T_{20}$ (24)	2.7	2.6	2.6	2.7
$T_{21}$ (22)	3.9	3.9	3.9	3.9
$T_{22}$ (20)	2.1	2.1	2.1	2.1
$E_{lab} = 3 \text{ MeV}$	AV18	AV18+LS1	AV18+LS2	AV18+LS3
$\sigma$ (37)	30.3	31.2	32.9	32.8
$A_y$ (38)	236.7	3.3	5.8	46.6
$iT_{11}$ (51)	149.1	10.4	3.9	14.8
$T_{20}$ (51)	4.4	2.7	3.0	3.2
$T_{21}$ (51)	6.8	5.0	4.4	4.5
$T_{22}$ (51)	12.7	14.8	14.8	14.3
$E_{lab} = 5 \text{ MeV}$	AV18	AV18+LS1	AV18+LS2	AV18+LS3
$\sigma$ (41)	29.3	30.2	30.2	30.5
$A_y$ (43)	229.8	6.9	8.5	38.5
$iT_{11}$ (61)	120.1	2.7	3.2	5.3
$T_{20}$ (61)	12.2	8.8	8.1	9.1
$T_{21}$ (61)	11.2	9.3	8.6	9.2
$T_{22}$ (61)	7.9	9.6	9.7	9.2
$E_{lab} = 10 \text{ MeV}$	AV18	AV18+LS1	AV18+LS2	AV18+LS3
$\sigma$ (42)	12.3	11.4	10.4	11.1
$A_y$ (48)	840.9	80.1	34.9	128.3
$iT_{11}$ (27)	37.3	4.2	3.1	4.9
$T_{20}$ (27)	12.8	8.4	6.7	7.9

$T_{21}$ (22)	6.3	3.9	3.5	4.0
$T_{22}$ (27)	25.4	29.8	32.0	29.4

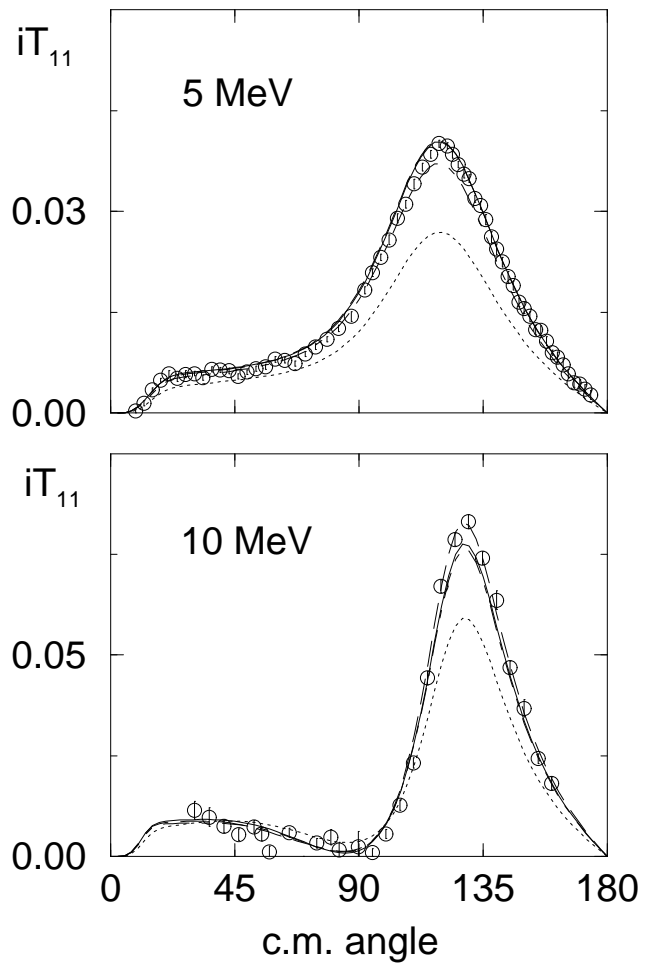
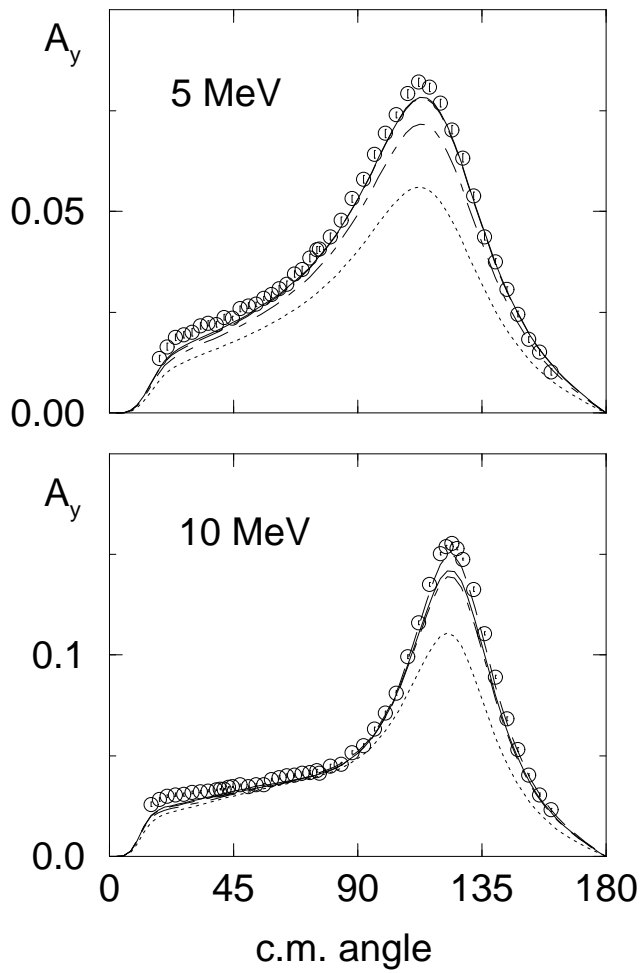
TABLE III.

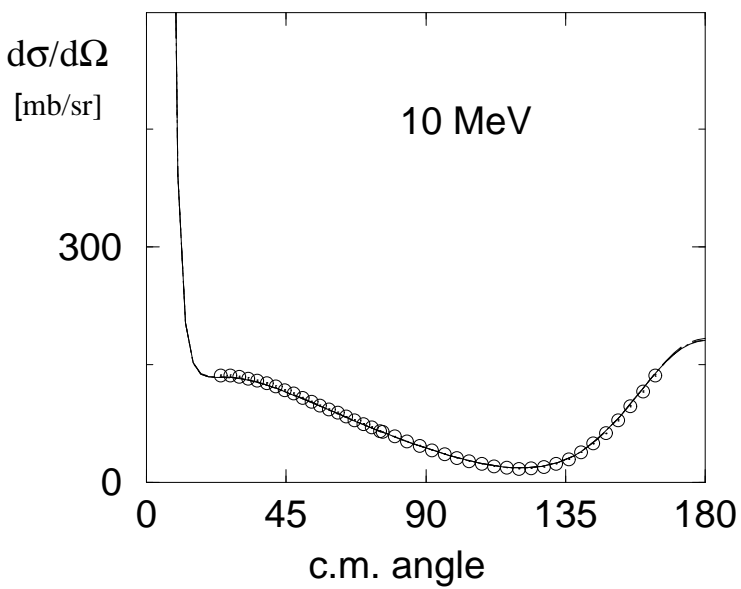
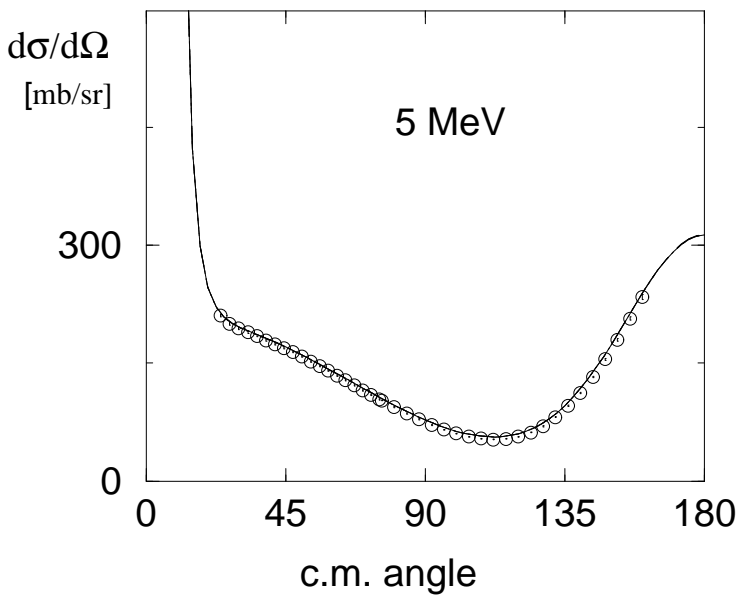
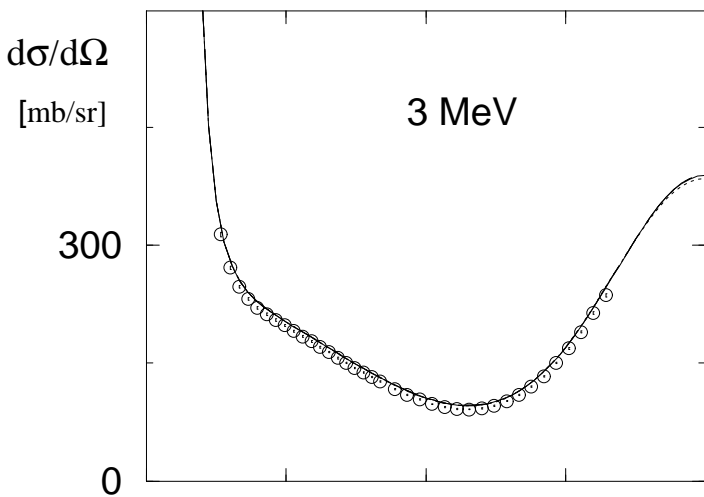
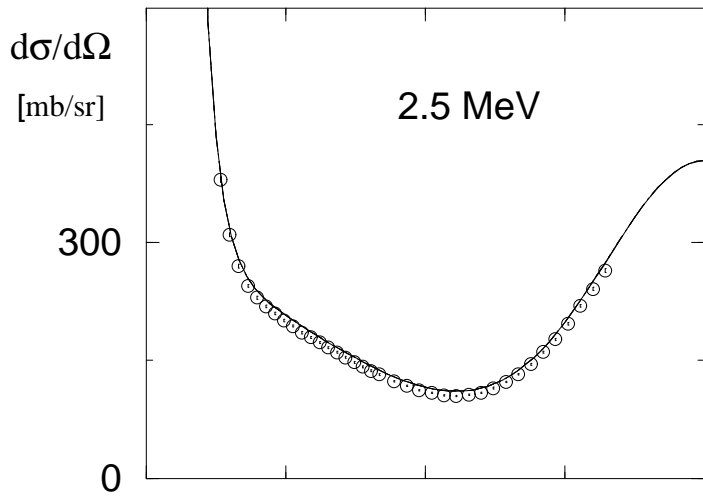
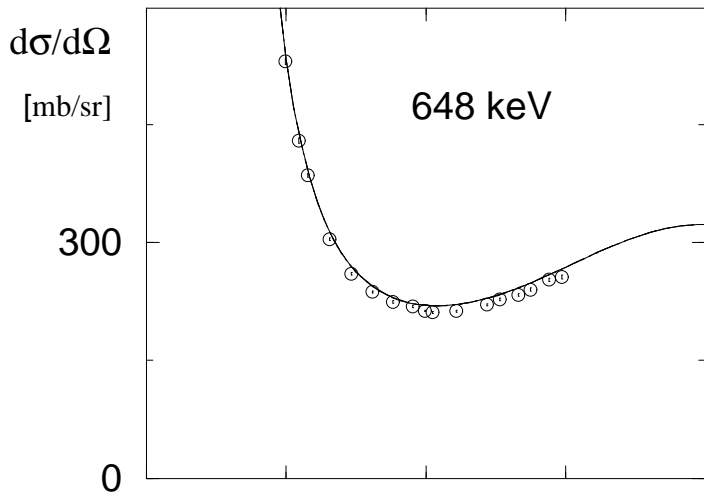


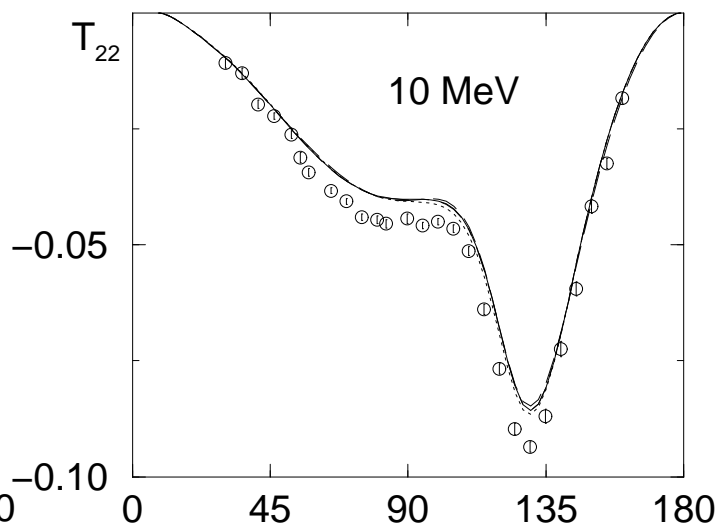
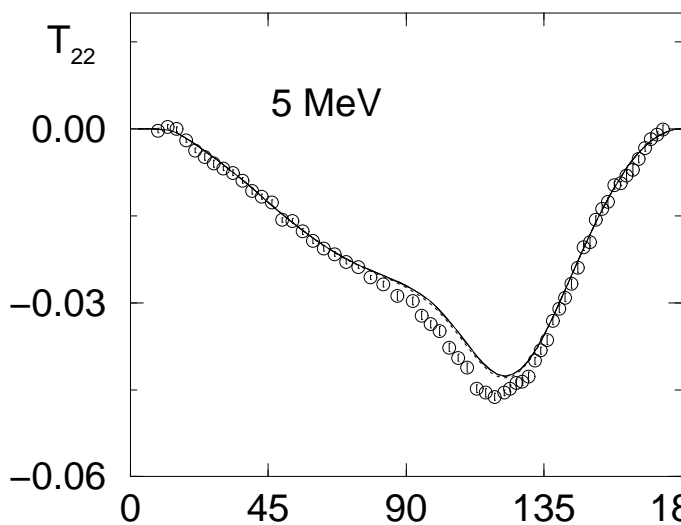
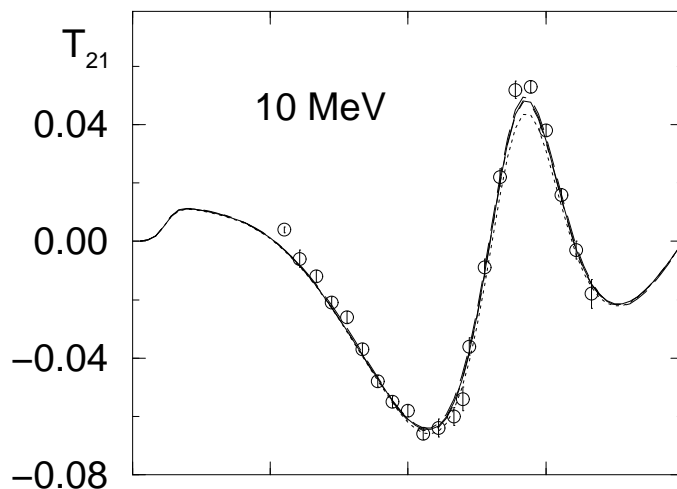
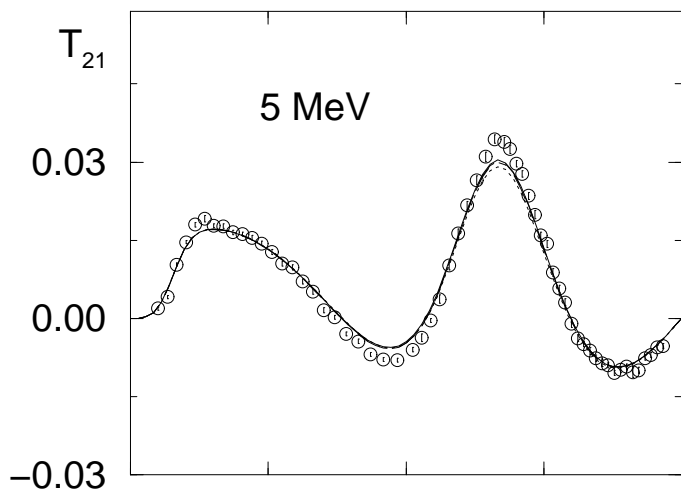
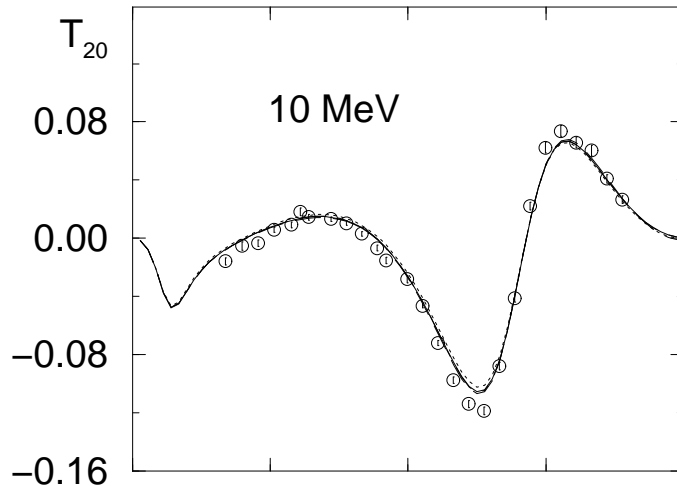
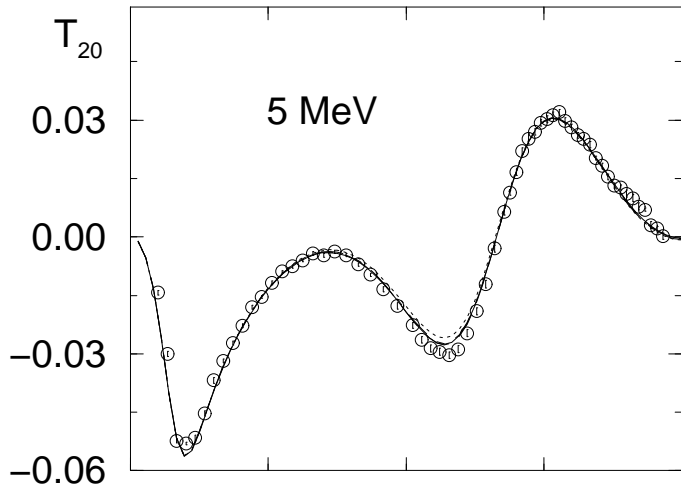












c.m. angle

c.m. angle